

Anisotropy in growth-front roughening

Y.-P. Zhao, G.-C. Wang, and T.-M. Lu

Department of Physics, Applied Physics, and Astronomy, and Center for Integrated Electronics and Electronics Manufacturing, Rensselaer Polytechnic Institute, Troy, New York 12180-3590

(Received 26 March 1998; revised manuscript received 14 August 1998)

We consider a linear anisotropic growth equation that includes two anisotropic physical processes, evaporation/condensation and surface diffusion, to describe the roughening of the growth fronts generated by noises. By solving this equation analytically, we show that there are two different types of growth-front anisotropy: correlation length anisotropy and scaling anisotropy. A scaling anisotropy can generate different values of roughness exponent in different surface directions. It is shown that a competition of the two growth processes can lead to a rotation of the direction of anisotropy. We also consider the effect of growth-front roughening due to the anisotropy in surface diffusion barrier (Schwoebel barrier) to show that the surface can form ripple structures over time. These results are used to explain recent experimental results on growth-front anisotropy. [S0163-1829(98)04544-5]

I. INTRODUCTION

Many surfaces in nature evolve under processes that add and/or remove materials, such as thin-film growth process, etching process, erosion, fracture, etc. These processes usually generate rough surfaces that can be described in terms of either self-affine fractal scaling, as a result of noise, or ‘‘mounds’’ formation due to the existence of surface diffusion barriers.^{1,2} These rough surfaces exhibit fluctuations in height normal to the surface. The fluctuations in height can be characterized in terms of the height-height correlation function $H(\mathbf{r}) = \langle [h(\mathbf{r}) - h(0)]^2 \rangle$. Here $h(\mathbf{r})$ is the surface height at position $\mathbf{r} = (x, y)$ on the surface. The notation $\langle \dots \rangle$ means an average over all possible choices of the origin, and an ensemble average over all possible surface configurations. Usually if an isotropic surface is assumed, by which the height-height correlation depends only on the magnitude of \mathbf{r} , then $H(r) \propto r^{2\alpha}$ for $r \ll \xi$, and $H(r) = \text{const}$ for $r \gg \xi$. Here ξ is the correlation length, within which the surface heights of any two points are correlated, and α is the roughness exponent. The value of α , which lies between zero and one, describes how wiggly the surface is. The smaller the α , the more wiggly the surface. The isotropic growth models fall into several universality classes with different values of roughness exponent.¹⁻⁸

However, in practice, sometimes surfaces may not be isotropic. Recent scanning tunneling microscopy (STM) study showed that the surface morphologies of homoepitaxial GaAs films on nominally flat GaAs(001) surfaces are highly anisotropic, with elongated multilayered features developing parallel to $[1\bar{1}0]$.⁹⁻¹² The anisotropy depends on the growth rate and substrate temperature.^{10,12} The height-height correlation functions along different directions are quite different.¹⁰ Similar morphologies have also been observed in metal-organic molecular-beam epitaxy (MOMBE) of InP on a nominally flat InP(100) substrate.¹³ The surface has a pattern with elongated structures along the $[0\bar{1}1]$ direction, and the surface anisotropy increases with time under the same growth condition. Anisotropic surface morphology also ex-

ists in heteroepitaxial films such as Ge/Si system.¹⁴ Recent study of $\text{In}_x\text{Al}_{1-x}\text{As}$ grown on InP(001) showed that the direction of the surface anisotropy could even rotate during the growth.¹⁵ Furthermore, anisotropy appeared in the growth of materials on stepped or vicinal surfaces. For example, it was observed that for Si grown on a vicinal Si(100) substrate with a 4° miscut, the surface morphology showed a strong shape anisotropy along the initial $[\bar{1}10]$ step direction.¹⁶

So far, theoretical description of the anisotropic growth phenomena has focused on nonlinear growth models. These include an anisotropic Kardar-Parisi-Zhang (KPZ) equation¹⁷⁻²⁰ and an anisotropic Kuramoto-Sivashinsky (KS) equation.²¹ One of the goals was to describe the growth on a stepped or a vicinal substrate. These pioneering works predict growth front morphology anisotropy, including anisotropic scaling. Quantitative predictions of these theories will be discussed later in this paper. Those nonlinear equations contain a term describing a growth direction normal to the local surface, which may not exist for some growth techniques such as molecular-beam epitaxy. Experimental work showed that, even when the growth started from a nominally flat substrate, anisotropic growth fronts could still be formed.^{9-13,16}

An important origin for the morphology anisotropy is due to the surface transport anisotropy. Several dynamic processes may be involved. The most important processes that affect the morphology are surface tension, surface diffusion, step barrier (Schwoebel barrier), and stress or strain on the surface. During thin-film growth, processes such as surface tension and surface diffusion tend to smooth the surface. For a vicinal surface, the surface tension depends on orientation.²² An anisotropic surface diffusion was also observed in the Si(100) substrate. The diffusion along the surface dimer rows is 1000 times faster than the diffusion across the dimer rows.²³⁻²⁵ Recent calculations on the step diffusion barrier of this surface also showed an anisotropy.²⁶ Surface strain or stress due to lattice mismatch or defects can induce surface diffusion; therefore, the anisotropic properties of surface stress or strain can cause surface anisotropy.²⁷

In general, a substrate anisotropy does not always lead to anisotropic growth unless it induces an anisotropic atomic transport. As an example, we consider the isotropic Edwards-Wilkinson (EW) growth,³ starting with anisotropic substrate morphology as the initial condition,

$$\frac{\partial h}{\partial t} = \nu \nabla^2 h + \eta(\mathbf{r}, t), \quad (1)$$

where ν is the surface tension, and $\eta(\mathbf{r}, t)$ is the Gaussian white noise. The solution for the power spectrum, which is defined as the Fourier transform of the surface autocovariance function $\langle h(\mathbf{r})h(0) \rangle$, is^{17,28}

$$P(\mathbf{q}, t) = 2D \frac{1 - e^{-2\nu q^2 t}}{\nu q^2} + P_0(\mathbf{q}) e^{-2\nu q^2 t}, \quad (2)$$

where $P_0(\mathbf{q})$ is the power spectrum of the anisotropic substrate, that is, from the initial surface morphology, which may be anisotropic. As time t increases, the effect of the substrate anisotropy becomes less important. For $t \rightarrow \infty$ the surface becomes isotropic because the contribution of the second term diminishes. Therefore, if there is no surface transport anisotropy the growth front started on an anisotropic substrate will eventually become isotropic after a long time.

In this paper we shall discuss a linear anisotropic growth model based on two common processes: evaporation/condensation (which gives rise to the surface tension term) and surface diffusion. We show that if only one of the physical processes is present in the growth equation the surface morphology can exhibit only a correlation length anisotropy, not a scaling anisotropy. The scaling anisotropy exists only when both processes take effect. The competition of these two effects sometimes may result in a rotation of the direction of anisotropy during growth. We also consider a similar linear growth model describing an anisotropic surface morphology as a result of an anisotropic step diffusion barrier on the surface.

II. LINEAR ANISOTROPIC SURFACE GROWTH MODEL

We first consider a noise-induced linear anisotropic growth model. We consider two main physical effects that can affect the surface morphology during growth: condensation/evaporation and surface diffusion. For condensation/evaporation the surface growth rate is proportional to the difference between the local surface chemical potential $\mu(\mathbf{r}, t)$ and the chemical potential of the vapor, $\bar{\mu}$.²⁹

$$\left. \frac{\partial h}{\partial t} \right|_{\text{cond}} = B[\mu(\mathbf{r}, t) - \bar{\mu}], \quad (3)$$

where B is a rate constant that depends on the equilibrium temperature, average vapor pressure, molecular weight, and molecular volume of the vapor.²⁹ According to Herring this chemical potential difference between a vapor and a thin film can be expressed as³⁰

$$\Delta\mu = \frac{1}{R_1} \left(\gamma + \frac{\partial^2 \gamma}{\partial n_1^2} \right) + \frac{1}{R_2} \left(\gamma + \frac{\partial^2 \gamma}{\partial n_2^2} \right), \quad (4)$$

where γ is the surface tension, R_1 and R_2 are the principal radii of surface curvature, n_1 and n_2 are the projections of the variable unit vector \mathbf{n} , on which γ depends, onto a plane tangent to the surface at the points in question. The subscripts 1 and 2 denote two perpendicular directions on the surface. If we assume that the two principal radii are parallel to the x and y axes, then for a slightly perturbed smooth surface, one has³¹

$$\left. \frac{\partial h}{\partial t} \right|_{\text{cond}} = B \left(\gamma_1 \frac{\partial^2 h}{\partial x^2} + \gamma_2 \frac{\partial^2 h}{\partial y^2} \right), \quad (5)$$

where $\gamma_i = \gamma + \partial^2 \gamma / \partial n_i^2$, $i = 1, 2$.

The effect of surface diffusion can be written as¹⁷

$$\left. \frac{\partial h}{\partial t} \right|_{\text{diff}} = -\nabla \cdot \mathbf{j}(\mathbf{r}, t), \quad (6)$$

where the current density $\mathbf{j} = (j_x, j_y, j_z = 0)$ is the surface diffusion flux. According to irreversible thermodynamics,

$$\mathbf{j}(\mathbf{r}, t) = \tilde{\mathbf{D}} \cdot \nabla \mu(\mathbf{r}, t). \quad (7)$$

Here $\tilde{\mathbf{D}}$ is the diffusion tensor,

$$\tilde{\mathbf{D}} = \begin{pmatrix} D_{xx} & D_{xy} & 0 \\ D_{yx} & D_{yy} & 0 \\ 0 & 0 & 0 \end{pmatrix}.$$

From Eqs. (3), (6), and (7), for a slightly perturbed smooth surface, one has

$$\begin{aligned} \left. \frac{\partial h}{\partial t} \right|_{\text{diff}} &= -\gamma_1 D_{xx} \frac{\partial^4 h}{\partial x^4} - \gamma_2 D_{yy} \\ &\times \frac{\partial^4 h}{\partial y^4} - (\gamma_2 D_{xx} + \gamma_1 D_{yy}) \frac{\partial^4 h}{\partial y^2 \partial x^2} \\ &- (D_{xy} + D_{yx}) \frac{\partial^2}{\partial x \partial y} \left(\gamma_1 \frac{\partial^2 h}{\partial x^2} + \gamma_2 \frac{\partial^2 h}{\partial y^2} \right). \end{aligned} \quad (8)$$

For a simple case, letting $D_{xy} = D_{yx} = 0$, one has

$$\begin{aligned} \left. \frac{\partial h}{\partial t} \right|_{\text{diff}} &= -\gamma_1 D_{xx} \frac{\partial^4 h}{\partial x^4} - \gamma_2 D_{yy} \frac{\partial^4 h}{\partial y^4} \\ &- (\gamma_2 D_{xx} + \gamma_1 D_{yy}) \frac{\partial^4 h}{\partial y^2 \partial x^2}. \end{aligned} \quad (9)$$

Combining Eqs. (5) and (9), and also considering the fluctuation of the flux of the arriving atoms during a deposition, we obtain a general growth equation as

$$\begin{aligned} \frac{\partial h}{\partial t} &= \nu_1 \frac{\partial^2 h}{\partial x^2} + \nu_2 \frac{\partial^2 h}{\partial y^2} - \kappa_1 \frac{\partial^4 h}{\partial x^4} \\ &- \kappa_2 \frac{\partial^4 h}{\partial y^4} - \kappa_3 \frac{\partial^4 h}{\partial x^2 \partial y^2} + \eta(\mathbf{r}, t), \end{aligned} \quad (10)$$

where $\nu_i = B \gamma_i$, $i = 1, 2$; $\kappa_1 = \gamma_1 D_{xx}$, $\kappa_2 = \gamma_2 D_{yy}$; and $\kappa_3 = \gamma_2 D_{xx} + \gamma_1 D_{yy}$. From now on we shall refer to the ν_i as the ‘‘surface tension,’’ and the κ_i as ‘‘surface diffusion.’’ $\eta(\mathbf{r}, t)$ is the Gaussian white noise, satisfying

$$\langle \eta(\mathbf{r}, t) \rangle = 0,$$

$$\langle \eta(\mathbf{r}_1, t_1) \eta(\mathbf{r}_2, t_2) \rangle = 2D \delta(\mathbf{r}_1 - \mathbf{r}_2) \delta(t_1 - t_2). \quad (11)$$

Equation (10) can be solved using a Fourier transform method.^{17,28,32} The solution for the power spectrum at time t is

$$P(\mathbf{q}, t) = 4D \frac{1 - \exp[-2(\nu_1 q_x^2 + \nu_2 q_y^2 + \kappa_1 q_x^4 + \kappa_2 q_y^4 + \kappa_3 q_x^2 q_y^2)t]}{\nu_1 q_x^2 + \nu_2 q_y^2 + \kappa_1 q_x^4 + \kappa_2 q_y^4 + \kappa_3 q_x^2 q_y^2}. \quad (12)$$

In the following, we consider three possible combinations of anisotropic surface tension and anisotropic surface diffusion in Eq. (12).

A. Surface tension only: $\kappa_i = 0, \nu_i \neq 0$

If the surface diffusion can be negligible, Eq. (12) becomes an anisotropic Edwards-Wilkinson equation with the power spectrum

$$P(\mathbf{q}, t) = 4D \frac{1 - \exp[-2(\nu_1 q_x^2 + \nu_2 q_y^2)t]}{\nu_1 q_x^2 + \nu_2 q_y^2}. \quad (13)$$

Let $Q_x = q_x t^{1/2}$, and $Q_y = q_y t^{1/2}$; Eq. (13) becomes

$$P(\mathbf{Q}, t)/t = 4D \frac{1 - \exp[-2(\nu_1 Q_x^2 + \nu_2 Q_y^2)]}{\nu_1 Q_x^2 + \nu_2 Q_y^2}. \quad (13')$$

Figure 1 plots the cross sections of the scaled power spectra $P(\mathbf{Q})/t$ in both the Q_x and Q_y directions and the contours of the scaled power spectra for $\nu_1 = 1.0$, $\nu_2 = 0.1$. For large q values the cross sections of the power spectra in both the Q_x and Q_y directions obey the same power law with the value of the power equal to -2 . This demonstrates that the roughness exponent $\alpha = 0$ through the relationship between α and slope: slope = $-d - 2\alpha$, where d is the dimension of the embedded space. Therefore α is not directionally dependent. However, the flat shoulder extends to different Q values in the Q_x and Q_y directions. The curve in the Q_y direction has its shoulder extend to $\sqrt{10}$ times further in Q values than that of the curve in the Q_x direction. This difference shows that the lateral scales ξ in these two directions are different; i.e., $\xi_x \cong \sqrt{10}\xi_y$. The lateral correlation lengths in the x and y directions equal $\sqrt{2\nu_1 t}$ and $\sqrt{2\nu_2 t}$, respectively; their ratio is $\sqrt{\nu_1/\nu_2}$. In fact if we do a linear transformation: $\sqrt{\nu_2/\nu_1} q_y \rightarrow q'_y$, $\sqrt{q_x^2 + q_y'^2} \rightarrow q'$; then Eq. (13) becomes isotropic,

$$P(\mathbf{q}', t) 4D \frac{1 - \exp[-2\nu_1 q'^2 t]}{\nu_1 q'^2}. \quad (14)$$

Therefore, except for the existence of an anisotropy in the lateral correlation length, the anisotropic EW equation has similar dynamic properties compared to that of the isotropic EW equation, e.g., $\beta = 0$, $\alpha = 0$, and $z = 2$ (see Table I).

B. Surface diffusion only: $\kappa_i \neq 0, \nu_i \approx 0$

If the surface tension contribution is negligible then Eq. (12) becomes an anisotropic Mullins-diffusion equation. The corresponding power spectrum is

$$P(\mathbf{q}, t) = 4D \frac{1 - \exp[-2(\kappa_1 q_x^4 + \kappa_2 q_y^4 + \kappa_3 q_x^2 q_y^2)t]}{\kappa_1 q_x^4 + \kappa_2 q_y^4 + \kappa_3 q_x^2 q_y^2}. \quad (15)$$

Let $Q_x = q_x t^{1/4}$, and $Q_y = q_y t^{1/4}$; Eq. (15) becomes

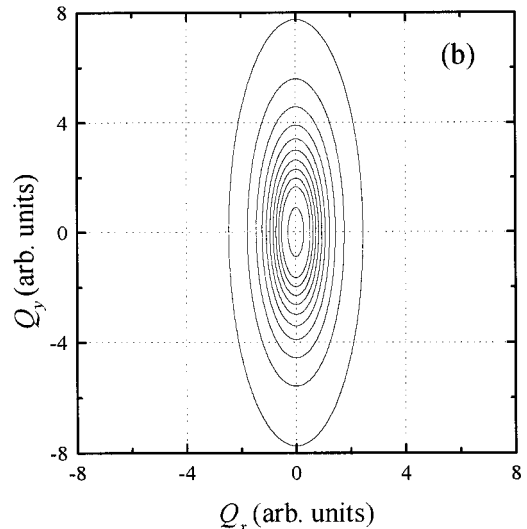
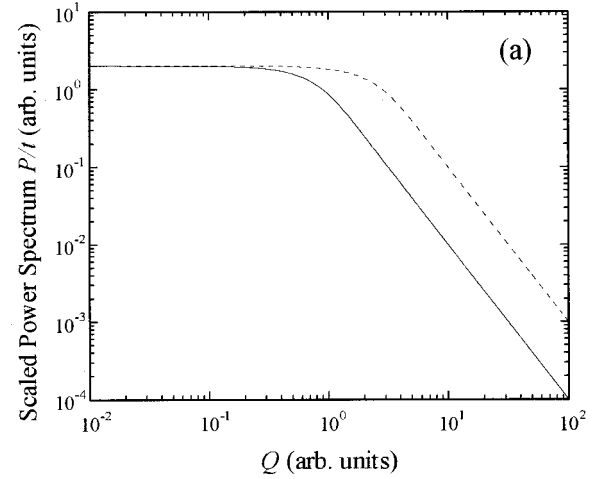


FIG. 1. (a) Log-log plots of the scaled power spectrum along the Q_x (solid curve) and Q_y (dashed curve) directions for $\nu_1 = 1.0$, $\nu_2 = 0.1$, $\kappa_1 = 0.0$, $\kappa_2 = 0.0$, and $\kappa_3 = 0.0$; (b) contour plots of the scaled power spectrum.

TABLE I. Summary of the surface properties of different anisotropic growth models.

Anisotropic Models	Conditions	Scaling Properties	Surface Properties	Ref.
	$\nu_1 \neq \nu_2, \kappa_1 = \kappa_2 = \kappa_3 = 0$	$\beta = 0, \alpha = 0, z = 2$	Correlation length anisotropy	
Linear model	$\nu_1 = \nu_2 = 0, \kappa_1 \neq \kappa_2 \neq \kappa_3$	$\beta = 0.25, \alpha = 1, z = 4$	Correlation length anisotropy	Present work
	$\nu_1 \neq 0, \nu_2 = 0, \kappa_1 = \kappa_3 = 0, \kappa_2 \neq 0$	$\beta = 0.125, \alpha_x = 0.25, \alpha_y = 0.5, z_y = 2z_x = 4$	Scaling anisotropy	
	$\nu_1 \neq \nu_2, \kappa_1 \neq \kappa_2 \neq \kappa_3$	$0 < \beta < 0.25, \alpha_x \neq \alpha_y$	Scaling anisotropy	
Linear model for step bias	$\frac{\nu_1}{\nu_2} < 0$		Ripple structures	Present work
	$\frac{\nu_1}{\nu_2} > 0, \nu_1 < 0$		Elliptical mounds	
	$\frac{\lambda_1}{\lambda_2} = 0$	$z_x \neq z_y$	Scaling anisotropy	
Kardar-Parisi-Zhang model	$\frac{\lambda_1}{\lambda_2} \neq 0$	$z_x = z_y = 2 - \alpha$	Correlation length anisotropy	18
	$\frac{\lambda_1}{\lambda_2} \neq 0$	$z_x = z_y = 2 - \alpha, \beta = 0.21, \alpha = 0.43$	Correlation length anisotropy	19
	$\frac{\lambda_1}{\lambda_2} < 0$	$\alpha_x = 0.25, \alpha_y = 0.75$	Scaling anisotropy	20
	$\frac{\nu_2}{\nu_1} > 0, \frac{\lambda_2}{\lambda_1} > 0$		Elliptical mounds	
Kuramoto-Sivashinsky model	$\frac{\nu_2}{\nu_1} < 0, \frac{\lambda_2}{\lambda_1} > 0$		Ripple structure	21
	$\frac{\lambda_2}{\lambda_1} < 0$		Ripple structure	

$$P(\mathbf{Q}, t)/t = 4D \frac{1 - \exp[-2(\kappa_1 Q_x^4 + \kappa_2 Q_y^4 + \kappa_3 Q_x^2 Q_y^2)]}{\kappa_1 Q_x^4 + \kappa_2 Q_y^4 + \kappa_3 Q_x^2 Q_y^2}. \quad (15')$$

The cross sections of the scaled power spectra $P(\mathbf{Q})/t$ in the Q_x and Q_y directions shown in Fig. 2 have a behavior similar to that of case A shown in Fig. 1, except that the value of the power is -4 , which leads to the same roughness exponent $\alpha = 1$ in the Q_x and Q_y directions. The shoulders extend to different values of Q due to the anisotropic diffusions in the x and y directions, which results in different values of ξ in the x and y directions. One can also perform a linear transformation by using $\sqrt{\kappa_2/\kappa_1} q_y \rightarrow q'_y, \sqrt{q_x^2 + q_y'^2} \rightarrow q'$ in Eq. (15) to make the power spectrum isotropic. Therefore, the dynamic behavior of the anisotropic Mullins diffusion equation is similar to that of the isotropic Mullins-diffusion equation, which gives $\beta = 0.25, \alpha = 1$, and $z = 4$ (see Table I).

Note that for either case A or case B the power-law behavior in the large q region is the same for both q_x and q_y directions; i.e., the scaling is isotropic. However, the lateral correlation length scale ξ is anisotropic. For equal values of ν_2/ν_1 in case A and κ_2/κ_1 in case B the anisotropy in case

A is more obvious than that in case B, as seen from the larger difference in the shoulder separation in case A.

C. General case: $\kappa_i \neq 0, \nu_i \neq 0$

One very interesting case involves the possibility that different physical processes dominate in different directions. For example, we consider what happens if the surface tension dominates in the x direction ($\nu_1 \gg \kappa_1$) while the surface diffusion dominates in the y direction ($\nu_2 \ll \kappa_2$). In this case the scaling forms [Eqs. (13') and (15')] do not exist. Figure 3 plots cross sections of the power spectra in both the q_x and q_y directions, and the contours of the power spectra for $\nu_1 = 1.0, \nu_2 = 0.1, \kappa_1 = 0.0, \kappa_2 = 4.0$, and $\kappa_3 = 40$ at different growth times. [Note that in Fig. 3(a) all the tails overlap for each q_x and q_y direction.] There are two notable features in Fig. 3. The power spectra along the q_x and q_y directions scale totally differently at large q , which gives different values of α . The anisotropy in the lateral correlation length still exists since the extension of the flat shoulders in the q_x and q_y directions are different. Initially the flat shoulder in the q_x direction is longer than the shoulder in the q_y direction. However, with the increase of growth time t the extension of

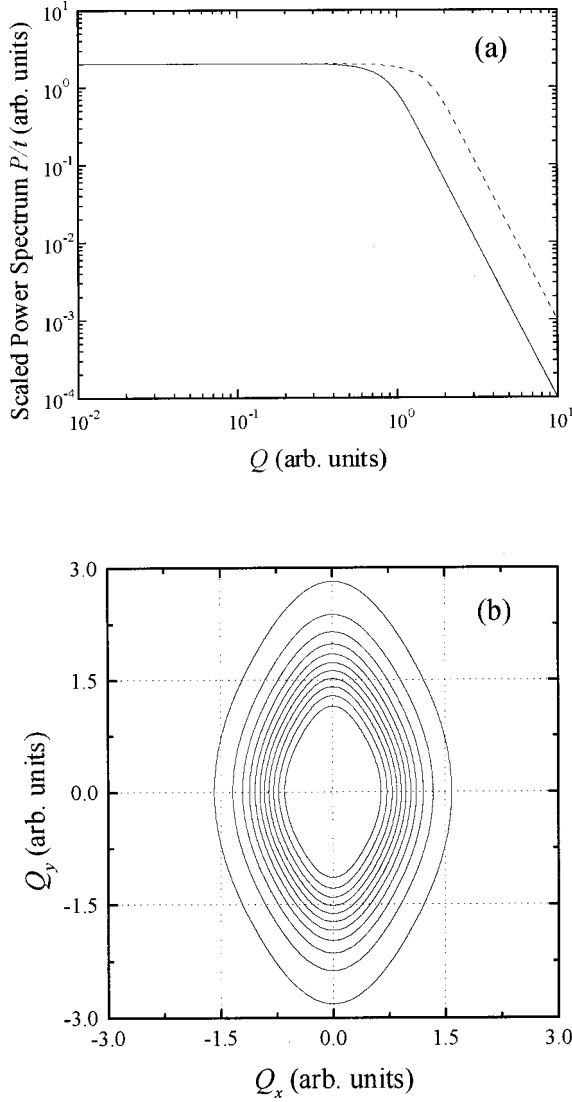


FIG. 2. (a) Log-log plots of scaled power spectrum along the Q_x (solid curve) and Q_y (dashed curve) directions for $\nu_1=0.0$, $\nu_2=0.0$, $\kappa_1=1.0$, $\kappa_2=0.1$, and $\kappa_3=1.1$; (b) contour plots of the scaled power spectrum.

the flat shoulders in the q_x and q_y directions becomes closer and closer. Then at a certain time ($t > 10$) the flat shoulder in the q_x direction becomes shorter than that of the q_y direction and we can see that the anisotropy of power spectra contours rotates 90° .

It is clear that in this case the x direction growth is dominated by the surface tension term and therefore the lateral correlation length ξ_x changes as $\xi_x = (2\nu_1 t)^{1/2}$. The y direction growth is governed by the surface diffusion and $\xi_y = (2\kappa_2 t)^{1/4}$. The anisotropic ratio is $\chi = \xi_x / \xi_y = (2\nu_1^2 / \kappa_2)^{1/4} t^{1/4}$. Initially for $t < 1$, the ratio $\chi < 1$. At time $t_c = k_2 / 2\nu_1^2$, $\chi = 1$. For a longer time $t > k_2 / 2\nu_1^2$, $\chi > 1$, the anisotropy rotates. This behavior can be used to explain qualitatively the rotation of anisotropy in $\text{In}_x\text{Al}_{1-x}\text{As}$ growth on $\text{InP}(001)$ observed by Sinn *et al.*¹⁵ For longer times, the anisotropic ratio increases as a power law of time, $\chi \propto t^{1/4}$, and the surface becomes more and more anisotropic. Under the condition of $\kappa_2 < 2\nu_1^2 t_c < 1$, one may not be able to observe the anisotropy rotation during the growth because the

transition time is very short. The surface morphology still has the scaling anisotropy, but the anisotropy does not rotate within the time scale considered.

The dynamic properties in this case would also change because different growth mechanisms govern the growth in different directions. Let us consider a very special case where $\nu_1 \neq 0$, $\nu_2 = 0$, $\kappa_1 = 0$, $\kappa_2 \neq 0$, and $\kappa_3 = 0$; Eq. (10) becomes

$$\frac{\partial h}{\partial t} = \nu_1 \frac{\partial^2 h}{\partial x^2} - \kappa_2 \frac{\partial^4 h}{\partial y^4} + \eta(\mathbf{r}, t). \quad (16)$$

Equation (16) states that the surface growth process is governed by surface tension in the x direction and by surface diffusion in the y direction. Use the scaling approach,

$$\begin{aligned} t &\rightarrow t' = bt, \\ h &\rightarrow h' = b^\beta h, \\ x &\rightarrow x' = b^{1/z_x} x, \\ y &\rightarrow y' = b^{1/z_y} y, \end{aligned} \quad (17)$$

Eq. (16) becomes

$$\begin{aligned} \frac{\partial h}{\partial t} &= \nu_1 b^{1-2/z_x} \frac{\partial^2 h}{\partial x^2} - \kappa_2 b^{1-4/z_y} \frac{\partial^4 h}{\partial y^4} \\ &+ b^{(1/2)-\beta-(1/2z_x)-(1/2z_y)} \eta(\mathbf{r}, t). \end{aligned} \quad (18)$$

Therefore, we obtain $\beta = 1/8$, $z_x = 2$, $z_y = 4$, and $\alpha_x = \beta z_x = 1/4$, $\alpha_y = \beta z_y = 1/2$. Note that the directionally dependent α values are quite different from those of both the EW model and the Mullins-diffusion model (see Table I).

In Fig. 4 we plot the interface width w as a function of growth time t through a numerical integration of Eq. (12) for specific cases of the three conditions discussed above: $\nu_1 = 1.0$, $\nu_2 = 0.1$, $\kappa_1 = 0.0$, $\kappa_2 = 4.0$, $\kappa_3 = 40$; $\nu_1 = 4.0$, $\nu_2 = 0.1$, $\kappa_1 = 0.0$, $\kappa_2 = 1.0$, $\kappa_3 = 40$; and $\nu_1 = 1.0$, $\nu_2 = 0$, $\kappa_1 = 0$, $\kappa_2 = 4.0$, $\kappa_3 = 0$. The values of the growth exponent β under these three conditions are about 0.20, 0.19, and 0.13, respectively. These β values lie between 0 (isotropic EW model) and 0.25 (isotropic Mullins-diffusion model). Here we should emphasize that for each condition there is only one β value for the growth even though the surface is anisotropic. However, the dynamic exponent $z = \alpha / \beta$ is directionally dependent for the anisotropic scaling case.

It is clear from the slopes in the tails of the power spectra that the anisotropic scaling surface can be formed only when two (or more) different anisotropic physical mechanisms (e.g., here condensation/evaporation and surface diffusion) are involved in the smoothing of the growth front. In different directions, different mechanisms would dominate. Using the argument of dynamic scaling, the lateral correlation length scales differently in different directions with time, $\xi_i \propto t^{z_i}$, and the height-height correlation function scales differently in different directions with different roughness exponents.

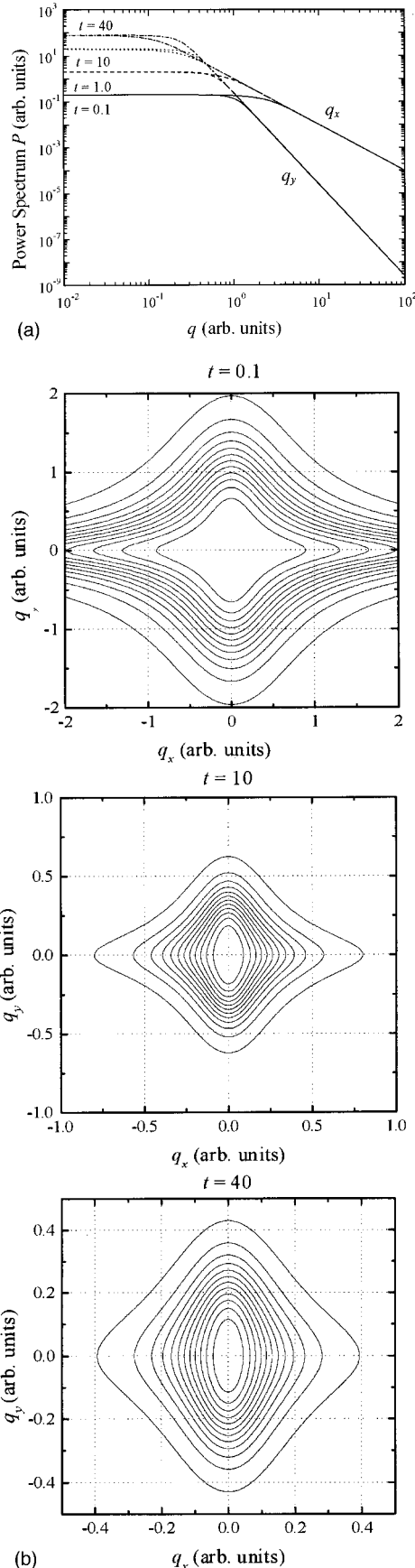


FIG. 3. (a) Log-log plots of power spectra along the q_x and q_y directions for $\nu_1=1.0$, $\nu_2=0.1$, $\kappa_1=0.0$, $\kappa_2=4.0$, and $\kappa_3=40$ at different growth times, $t=0.1$, 10, and 40; (b) contour plots of the power spectra at different growth times.

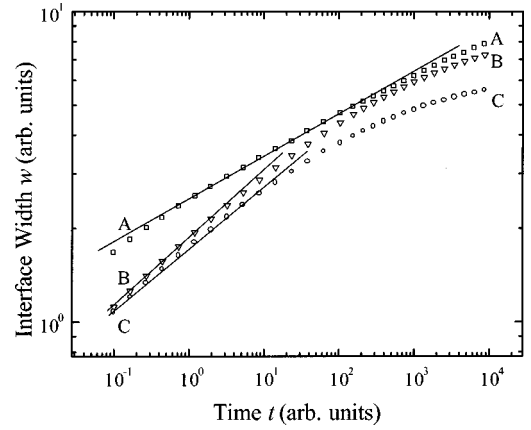


FIG. 4. Interface width w as a function of growth time t for A: $\nu_1=1.0$, $\nu_2=0$, $\kappa_1=0$, $\kappa_2=4.0$, and $\kappa_3=0$. B: $\nu_1=1.0$, $\nu_2=0.1$, $\kappa_1=0.0$, $\kappa_2=4.0$, and $\kappa_3=40$. C: $\nu_1=4.0$, $\nu_2=0.1$, $\kappa_1=0.0$, $\kappa_2=1.0$, and $\kappa_3=40$.

III. STEP BARRIER ANISOTROPY

In the presence of a Schwoebel barrier, the step barriers prevent adatoms from hopping down the step edge, which generates an uphill diffusion current.^{33–39} In this case the surface consists of regular mound structures. After an initial transient the slope of the mounds remains essentially constant, giving a slope selection.³⁴ This isotropic growth mechanism can be described by a nonlinear Langevin equation proposed by Johnson *et al.*,³³

$$\frac{\partial h(\mathbf{r}, t)}{\partial t} = -\nu \nabla \frac{\nabla h}{1 + (\nabla h)^2} - \kappa \nabla^4 h + \eta(\mathbf{r}, t), \quad (19)$$

where both ν and κ are positive. The first term on the right-hand side represents the uphill growth due to the Schwoebel barrier effect, and the second term is due to the surface diffusion. The up/down symmetry is still preserved for this equation although it is nonlinear. An example of the isotropic step barrier induced coarsening was the growth of Cu/Cu(100).³⁹ However, in GaAs/GaAs(100) growth, an anisotropy in the morphology was observed.^{9–12} Considering an anisotropic growth, Eq. (19) can be written as

$$\begin{aligned} \frac{\partial h(\mathbf{r}, t)}{\partial t} = & -\nu_1 \frac{\partial}{\partial x} \frac{\partial h / \partial x}{1 + (\partial h / \partial x)^2} + \nu_2 \frac{\partial^2 h}{\partial y^2} - \kappa_1 \frac{\partial^4 h}{\partial x^4} - \kappa_2 \frac{\partial^4 h}{\partial y^4} \\ & - \kappa_3 \frac{\partial^4 h}{\partial x^2 \partial y^2} + \eta(\mathbf{r}, t). \end{aligned} \quad (20)$$

Here ν_1 and ν_2 have different meanings. The ν_1 represents the uphill growth due to the Schwoebel barrier effect, but the ν_2 represents the surface tension. Equation (20) demonstrates that the growth in the x direction is governed by step barriers while in the y direction the growth is dominated by condensation/evaporation. Equation (20) can be linearized as

$$\begin{aligned} \frac{\partial h}{\partial t} = & -\nu_1 \frac{\partial^2 h}{\partial x^2} + \nu_2 \frac{\partial^2 h}{\partial y^2} - \kappa_1 \frac{\partial^4 h}{\partial x^4} - \kappa_2 \frac{\partial^4 h}{\partial y^4} - \kappa_3 \frac{\partial^4 h}{\partial x^2 \partial y^2} \\ & + \eta(\mathbf{r}, t). \end{aligned} \quad (21)$$

Equation (21) is similar to Eq. (12), except that there is a negative sign before ν_1 . This negative term would cause an

unstable growth in the x direction, and would dominate the surface growth in long time since the growth in the y direction is stable. Figure 5 plots the cross sections of the power spectra in both the q_x and q_y directions, and the contours of the power spectra for $\nu_1 = -1.0$, $\nu_2 = 0.1$, $\kappa_1 = 1.0$, $\kappa_2 = 0.1$, and $\kappa_3 = 1.1$ at different growth times. Initially the power spectrum is anisotropic without a maximum peak ($t = 0.1$). But for later times a peak gradually forms in the q_x direction and becomes more and more pronounced ($t \geq 1.0$). This is evidence of the wavelength selection. After a certain growth time ($t > 10$), this peak in the q_x direction dominates the power spectrum, and the surface begins to form a ripple structure. After a long time the surface forms one-dimensional periodic stripes. Such a ripple structure was observed in systems having Schwoebel diffusion barriers that we believe to possess anisotropy. One such example is the growth of GaAs.⁹⁻¹²

If two orthogonal directions have different barrier heights, Eq. (20) can be written as

$$\begin{aligned} \frac{\partial h(\mathbf{r}, t)}{\partial t} = & -\nu_1 \frac{\partial}{\partial x} \frac{\partial h / \partial x}{1 + (\partial h / \partial x)^2} - \nu_2 \frac{\partial}{\partial y} \frac{\partial h / \partial y}{1 + (\partial h / \partial y)^2} \\ & - \kappa_1 \frac{\partial^4 h}{\partial x^4} - \kappa_2 \frac{\partial^4 h}{\partial y^4} - \kappa_3 \frac{\partial^4 h}{\partial x^2 \partial y^2} + \eta(\mathbf{r}, t). \end{aligned} \quad (22)$$

This equation would produce an elliptical mound structure.

IV. DISCUSSIONS

From the above discussion we see that a noise induced surface morphology can be described by at least two different anisotropies: correlation length anisotropy and scaling anisotropy. In the correlation length anisotropy the linear dynamic growth equation can be made isotropic by a linear transformation. In this case, the formation of the lateral anisotropic surface can be simply achieved by stretching an isotropic surface in certain directions, affecting different lateral correlation lengths. The scaling properties of the surface would remain the same in all directions. From the point of view of dynamic growth, such a kind of surface is the result of only one dominant anisotropic surface process during growth.

In the case of anisotropic scaling the roughness exponent α is directional dependent, with or without a correlation length anisotropy. In this case the surface is formed by at least two surface processes, of which at least one is anisotropic. The overall interface width of the surface scales with the growth time as t^β , which means that the values of dynamic exponent z in different directions are different. This may lead to a rotation of the anisotropy, which has been observed experimentally.

The step barrier anisotropy can also generate an anisotropic surface. In this case, initially the surface is a random rough surface with or without anisotropy. But with an increase of the growth time, the surface can form ripple structures, and eventually would form periodic stripes. We have shown that these features can be obtained from a simple linearized growth equation including the effect of a step barrier anisotropy.

Quantitative predictions of the scaling properties and growth exponents for the linear growth models are summa-

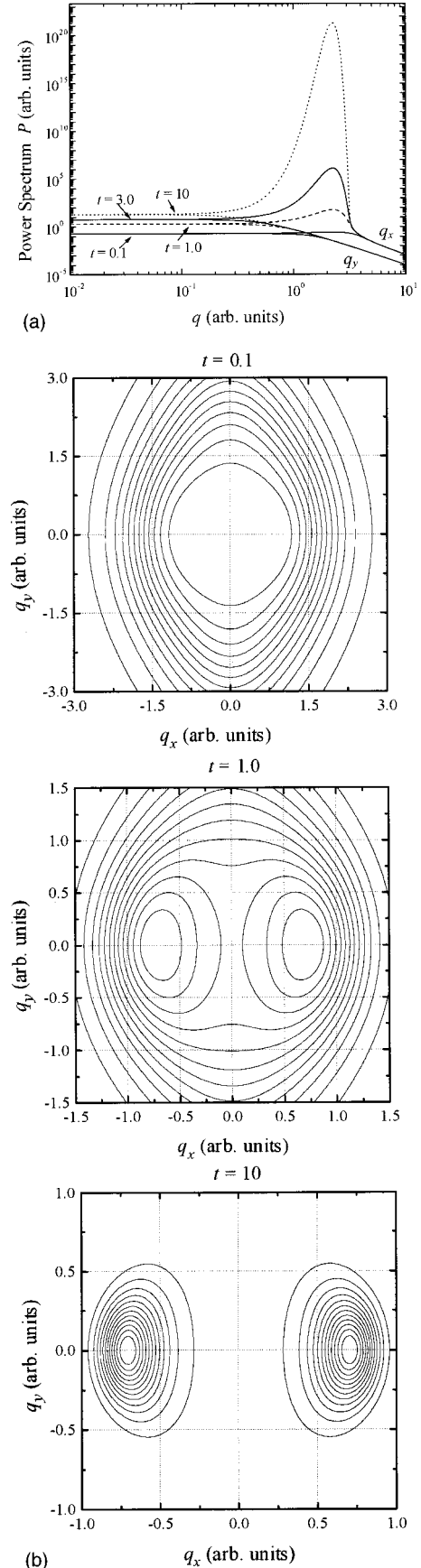


FIG. 5. (a) Log-log plots of power spectra along the q_x and q_y directions for $\nu_1 = -1.0$, $\nu_2 = 0.1$, $\kappa_1 = 1.0$, $\kappa_2 = 0.1$, and $\kappa_3 = 1.1$ at different growth times, $t = 0.1, 1.0$, and 10 ; (b) contour plots of the power spectra at different growth times.

rized in Table I. For a comparison, we also list in the same table the results predicted by existing nonlinear theories. The highlights of these theories are in the following.

An anisotropic KPZ equation^{17,18} can be written as

$$\frac{\partial h}{\partial t} = \nu_1 \frac{\partial^2 h}{\partial x^2} + \nu_2 \frac{\partial^2 h}{\partial y^2} + \frac{\lambda_1}{2} \left(\frac{\partial h}{\partial x} \right)^2 + \frac{\lambda_2}{2} \left(\frac{\partial h}{\partial y} \right)^2 + \eta(\mathbf{r}, t). \quad (23)$$

As discussed by Wolf, the surface anisotropy is characterized by two correlation lengths ξ_x and ξ_y , which have the relationship $\xi_x = \xi_y^\chi$, where χ is an anisotropic exponent.¹⁸ Through a renormalization argument, he also demonstrated that in the case $\lambda_1/\lambda_2 \neq 0$, $\chi = 1$, and $z + \alpha = 2$, where $z = \alpha/\beta$ is a dynamic exponent; if $\lambda_1/\lambda_2 = 0$, then $\chi \neq 1$ and $z = 2\chi = 2 - \alpha$. Barabási, Araujo, and Stanley showed numerically that $\alpha = 0.43, \beta = 0.21$.¹⁹ However, based on a restricted solid-on-solid (RSOS) model, Jeong, Kahng, and Kim showed that when $\lambda_1 > 0$ and $\lambda_2 < 0$, the anisotropic KPZ equation gives directionally dependent roughness exponents, $\alpha_x = 0.25$ and $\alpha_y = 0.75$ in two orthogonal directions.²⁰

Rost and Krug also investigated the anisotropic KS equation,²¹

$$\frac{\partial h}{\partial t} = -\nu_1 \frac{\partial^2 h}{\partial x^2} - \nu_2 \frac{\partial^2 h}{\partial y^2} - \kappa (\nabla^2)^2 h + \frac{\lambda_1}{2} \left(\frac{\partial h}{\partial x} \right)^2 + \frac{\lambda_2}{2} \left(\frac{\partial h}{\partial y} \right)^2 + \eta(\mathbf{r}, t), \quad (24)$$

where $\nu_1 > 0, \lambda_1 > 0$. They found that if $\lambda_2/\lambda_1 > \min(0, \nu_2/\nu_1)$, the nonlinearities stabilized the linear instability, leading to a state of bounded spatiotemporal chaos. If $\nu_2/\nu_1 < 0$ and $\lambda_2/\lambda_1 > 0$, the growth front initially dominates by ripples running parallel to the y axis, but evolves into an anisotropic cellular chaotic state for long time, and the ripples pinch off. If $\lambda_2/\lambda_1 < \min(0, \nu_2/\nu_1)$, the growth front is dominated by domains of connected ripples. The domain size and the ripple amplitude increase as power laws of time.²¹

Experimentally, although a large body of work has shown the existence of roughness anisotropy in growth fronts, very little quantitative measurement has been reported on the growth parameters listed in Table I. Therefore, at this time, it is difficult to assess the validity of these models for different experimental systems. It is hope that our work will stimulate more experimental work in the study of anisotropic growth fronts.

ACKNOWLEDGMENTS

This work was supported by the NSF. The authors thank J. B. Wedding and M. Stowe for reading the manuscript.

-
- ¹For a review, see *Dynamics of Fractal Surfaces*, edited by F. Family and T. Vicsek (World Scientific, Singapore, 1990).
- ²A.-L. Barabási and H. E. Stanley, *Fractal Concepts in Surface Growth* (Cambridge University Press, New York, 1995).
- ³S. F. Edwards and D. R. Wilkinson, Proc. R. Soc. London, Ser. A **381**, 17 (1982).
- ⁴D. E. Wolf and J. Villain, Europhys. Lett. **13**, 389 (1990).
- ⁵S. Das Sarma and P. Tamborenea, Phys. Rev. Lett. **66**, 325 (1991).
- ⁶L. Golubovic and R. Bruinsma, Phys. Rev. Lett. **66**, 321 (1991).
- ⁷M. Kardar, G. Parisi, and Y.-C. Zhang, Phys. Rev. Lett. **56**, 899 (1986).
- ⁸Rodolfo Cuerno and Kent Bækgaard Lauritsen, Phys. Rev. E **52**, 4853 (1995).
- ⁹E. J. Heller and M. G. Lagally, Appl. Phys. Lett. **60**, 2675 (1992).
- ¹⁰R. Maboudian, V. Bressler-Hill, K. Pond, X.-S. Wang, P. M. Petroff, and W. H. Weinberg, Surf. Sci. **302**, L269 (1994).
- ¹¹C. Orme, M. D. Johnson, J. L. Sudijono, K. T. Leung, and B. G. Orr, Appl. Phys. Lett. **64**, 860 (1994).
- ¹²A. J. Pidduck, G. W. Smith, A. M. Keir, and C. R. Whitehouse, in *Mechanisms of Thin Film Evolution*, edited by S. M. Yalisove, C. V. Thompson, and D. J. Eaglesham, MRS Symposia Proceedings No. 317 (Materials Research Society, Pittsburgh, 1994), p. 53.
- ¹³M. A. Cotta, R. A. Hamm, T. W. Staley, S. N. G. Chu, L. R. Harriott, M. B. Panish, and H. Temkin, Phys. Rev. Lett. **70**, 4106 (1993).
- ¹⁴R. L. Headrick, J.-M. Baribeau, and Y. E. Strausser, Appl. Phys. Lett. **66**, 96 (1995).
- ¹⁵M. T. Sinn, J. A. del Alamo, B. R. Bennett, K. Haberman, and F. G. Celii, J. Electron. Mater. **25**, 313 (1996).
- ¹⁶N.-E. Lee, D. G. Cahill, and J. E. Greene, Phys. Rev. B **53**, 7876 (1996).
- ¹⁷J. Villain, J. Phys. I **1**, 19 (1991).
- ¹⁸D. E. Wolf, Phys. Rev. Lett. **67**, 1783 (1991).
- ¹⁹A. L. Barabasi, M. Araujo, and H. E. Stanley, Phys. Rev. Lett. **68**, 3729 (1992).
- ²⁰H. Jeong, B. Kahng, and D. Kim, Phys. Rev. Lett. **77**, 5094 (1996).
- ²¹M. Rost and J. Krug, Phys. Rev. Lett. **75**, 3894 (1995).
- ²²J. B. Hudson, *Surface Science, An Introduction* (Butterworth-Heinemann, Boston, 1992).
- ²³Y.-W. Mo, B. S. Swartzentruber, R. Kariotis, M. B. Webb, and M. G. Lagally, Phys. Rev. Lett. **63**, 2393 (1989); Y. W. Mo, J. Kleiner, M. B. Webb, and M. G. Lagally, *ibid.* **66**, 1998 (1991).
- ²⁴R. J. Hamers, U. K. Kohler, and J. E. Demuth, J. Vac. Sci. Technol. A **8**, 195 (1990).
- ²⁵B. Voigtlander, T. Weber, P. Smilauer, and D. E. Wolf, Phys. Rev. Lett. **78**, 2164 (1997).
- ²⁶S. Kodiyalam, K. E. Khor, and S. Das Sarma, Phys. Rev. B **53**, 9913 (1996).
- ²⁷D. J. Srolovitz, Acta Metall. **37**, 621 (1989); L. B. Freund, G. E. Beltz, and F. Jonsdottir, in *Thin Films: Stresses and Mechanical Properties IV*, edited by K. Rodbell, B. Filter, H. Frost, and P. Ho, MRS Symposia Proceedings No. 308 (Materials Research Society, Pittsburgh, 1993), p. 383; C. Roland and G. H. Gilmer, Phys. Rev. B **46**, 13 428 (1992); **46**, 13 437 (1992).
- ²⁸S. Majaniemi, T. Ala-Nissila, and J. Krug, Phys. Rev. B **53**, 8071 (1996).
- ²⁹W. W. Mullins, J. Appl. Phys. **28**, 333 (1957).
- ³⁰C. Herring, in *The Physics of Powder Metallurgy*, edited by W. E. Kingston (McGraw-Hill, New York, 1951), Chap. 8, pp. 143.

- ³¹A. W. Nutbourne and R. R. Martin, *Differential Geometry Applied to Curve and Surface Design* (Ellis Horwood, Chichester, England, 1988).
- ³²Y.-P. Zhao, H.-N. Yang, G.-C. Wang, and T.-M. Lu, Phys. Rev. B **57**, 1922 (1998).
- ³³M. D. Johnson, C. Orme, A. W. Hunt, D. Graff, J. Sudijono, L. M. Sander, and B. G. Orr, Phys. Rev. Lett. **72**, 116 (1994).
- ³⁴M. Siegert and M. Plischke, Phys. Rev. Lett. **73**, 1517 (1994).
- ³⁵P. E. Hegeman, H. J. W. Zandvliet, G. A. M. Kip, and A. van Silfhout, Surf. Sci. **311**, L655 (1994).
- ³⁶J. A. Stroschio, D. T. Pierce, M. D. Stiles, A. Zangwill, and L. M. Sander, Phys. Rev. Lett. **75**, 4246 (1995).
- ³⁷J. E. Van Nostrand, S. J. Chey, M.-A. Hasan, D. G. Cahill, and J. E. Greene, Phys. Rev. Lett. **74**, 1127 (1995).
- ³⁸F. Tsui, J. Wellman, C. Uher, and R. Clarke, Phys. Rev. Lett. **76**, 3164 (1996).
- ³⁹J.-K. Zuo and J. F. Wendelken, Phys. Rev. Lett. **78**, 2791 (1997).